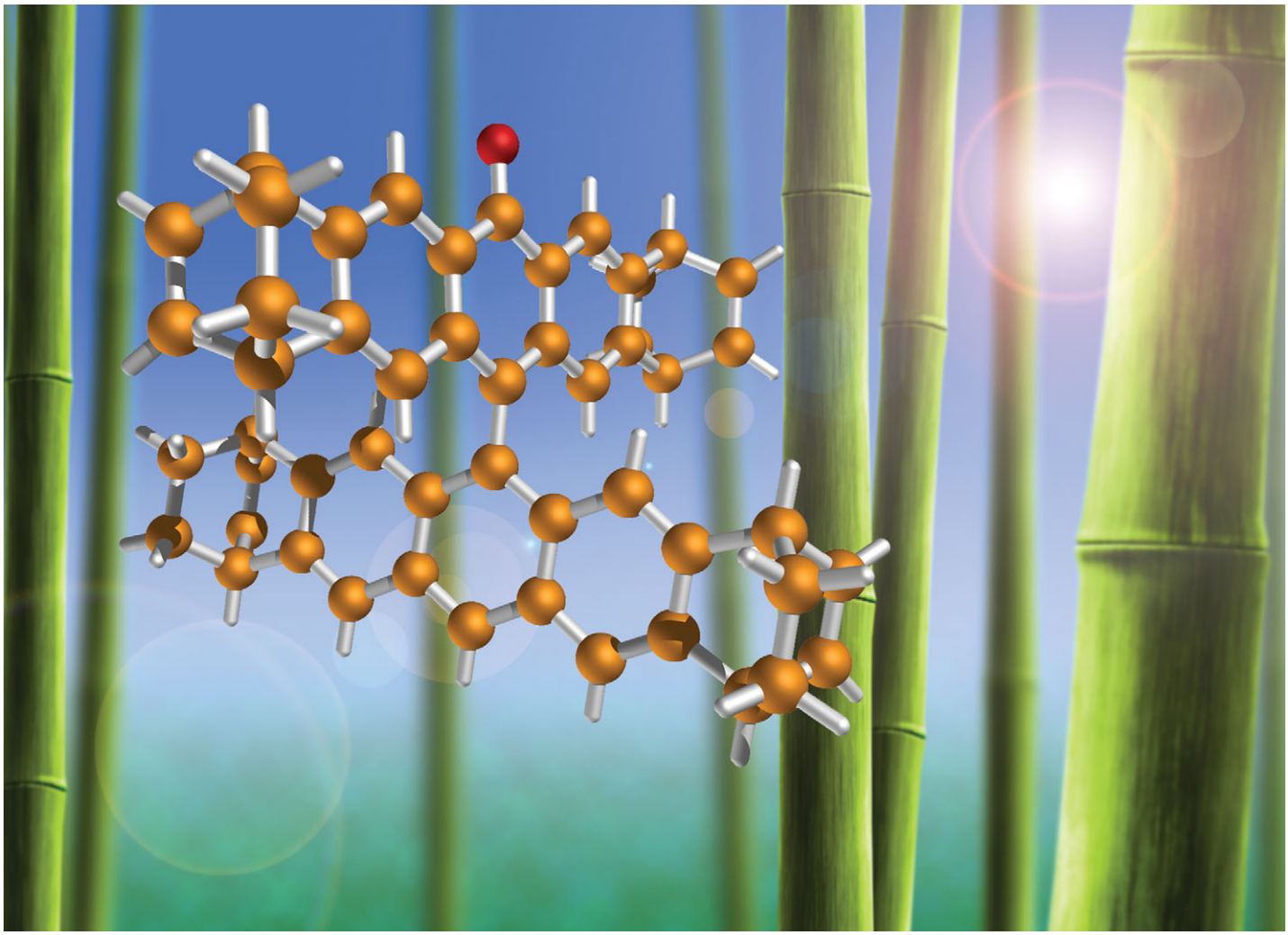

Showcasing work from the laboratories of Jishan Wu (National University of Singapore (NUS), Singapore), Tsuyoshi Kawai and Hiroko Yamada (Nara Institute of Science and Technology (NAIST), Japan).

9,9′-Anthryl-anthroxyl radicals: strategic stabilization of highly reactive phenoxyl radicals

Stable 9,9′-anthryl-anthroxyl radicals were synthesized and fully characterized. Owing to the stabilization by resonance and steric effects, one of the radicals showed an extremely long half-life of 11 days in solution.

As featured in:

See Jishan Wu, Hiroko Yamada *et al.*, *Chem. Commun.*, 2015, **51**, 6734.

ROYAL SOCIETY OF CHEMISTRY

www.rsc.org/chemcomm

Registered charity number: 207890

ChemComm

COMMUNICATION

View Article Online
View Journal | View Issue

Cite this: *Chem. Commun.*, 2015, 51, 6734

Received 18th December 2014,
Accepted 27th January 2015

DOI: 10.1039/c4cc10104a

www.rsc.org/chemcomm

9,9′-Anthryl-anthroxyl radicals: strategic stabilization of highly reactive phenoxyl radicals†

Tatsuya Aotake,[a] Mitsuharu Suzuki,[a] Naoki Aratani,[a] Junpei Yuasa,[a] Daiki Kuzuhara,[a] Hironobu Hayashi,[a] Haruyuki Nakano,[b] Tsuyoshi Kawai,[a] Jishan Wu*[c] and Hiroko Yamada*[ad]

Stable 9,9′-anthryl-anthroxyl radicals were synthesized and isolated, and the structures were fully characterized by single crystal X-ray diffraction analysis and ESR measurement. The resonance structure and steric protection of the peripheral positions and the most reactive 9-position of anthracene prolong the half-life of the radical in solution to 11 days.

Phenoxyl radical,[1] which is one of the highly reactive radicals, is observed in biological processes as a tyrosyl radical related to electron transfer, hydrogen atom transfer and proton-coupled electron transfer.[2] It formally contains resonance structure, as shown in Scheme 1, in which the carbon atom at the 4-position is also reactive. The stabilization has been achieved by substitution with bulky *ortho*-substituents,[3] coordination to metal ions[4] or π-conjugation expansion.[5]

During the synthetic investigation of molecular graphene nano-ribbons (GNRs),[6] we found the formation of a stable anthroxyl radical. The preparation of 9,9′-anthryl-anthr-10-oxy radical (**1**), an example of a π-expanded phenoxyl radical, was reported by Singer *et al.* in 1971, where **1** was obtained by the oxidation of 9,9′-bianthryl by molecular oxygen, but only the hyperfine coupling constants (hfccs) and *g*-value were reported without an ESR spectrum.[7] Here, we will report the synthesis and characterization of stable radical **1**, including the direct comparison of **1** and 10-hydroxy-9,9′-anthrylanthracene (**1-H**),

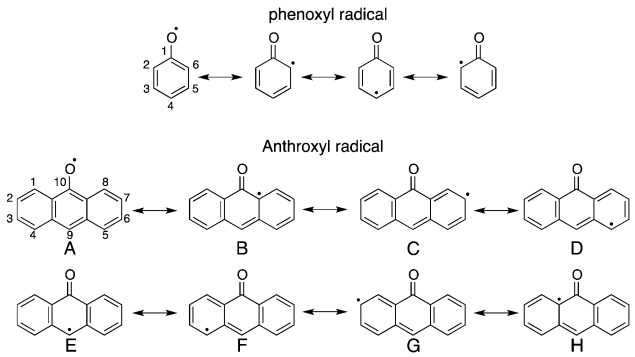

Scheme 1 Resonance structures of phenoxyl radical and anthroxyl radical.

using the X-ray single crystal structure analysis of the co-crystal of **1** and **1-H**. We have also prepared tetrabicyclo[2.2.2]octadiene (BCOD)-fused 9,9′-anthryl-anthr-10-oxy radical derivative **2** as a more stabilized radical species under ambient conditions. The stability of the compound **2** was attained by two factors. One is the expansion of the π-structure as same as radical **1**: the expansion of the phenyl skeleton expanded to anthracene, resulting in the gain of two aromatic stabilization energies as shown in Scheme 1, the other is *ortho* substitution of bulky substituents at periphery and the most reactive 9-position. Thus the radical **2** is stable enough to be purified over a conventional silica gel column.

The synthetic route of **1** and **2** is shown in Scheme 2. Bisanthracene quinones **3** and **4** were prepared according to the literature.[8,9] Hydride reduction of **3** and **4** using lithium aluminium hydride (LAH) and 6 N HCl produced monoketones **5** and **6**, respectively. The monoketones were used in the following reaction without purification because of the instability under ambient conditions. The radicals **1** and **2** were obtained by the treatment of monoketones with pyridine *N*-oxide and $FeSO_4 \cdot 7H_2O$ in 15% and 19% yield in 2 steps, respectively. The products were identified by mass spectrum measurement (Fig. S1–S3, ESI†), single crystal X-ray diffraction analysis and ESR spectroscopy.

[a] *Graduate School of Materials Science, Nara Institute of Science and Technology (NAIST), 8916-5 Takayama-cho, Ikoma 630-0192, Japan. E-mail: hyamada@ms.naist.jp*
[b] *Department of Chemistry, Graduate School of Sciences, Kyushu University, Fukuoka 812-8581, Japan*
[c] *National University of Singapore, 3 Science Drive 3, 117543, Singapore. E-mail: chmwuj@nus.edu.sg*
[d] *CREST, Japan Science and Technology Agency (JST) 4-1-8 Honcho, Kawaguchi, Saitama 332-0012, Japan*

† Electronic supplementary information (ESI) available: Synthetic details, X-ray crystal structural analysis, DFT calculations, time profiles of UV-vis absorption spectra, and thermal analysis. CCDC 1021762 (**1**), 1021763 (**1** and **1-H**), and 1021764 (**2**). For ESI and crystallographic data in CIF or other electronic format see DOI: 10.1039/c4cc10104a

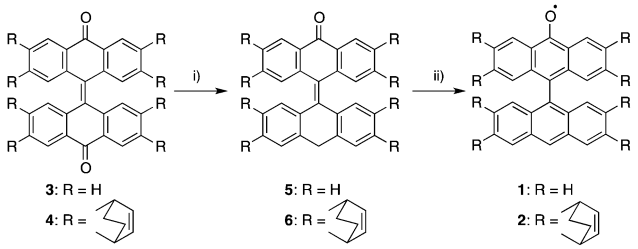

Scheme 2 Syntheses of **1** and **2**: (i) lithium aluminium hydride (LAH), dry THF, then 6 N HCl, reflux; (ii) $FeSO_4{\cdot}7H_2O$, pyridine-*N*-oxide, pyridine, piperidine, 100 °C.

The single crystals were obtained by diffusion crystallization with chloroform/methanol for **1**, and the crystallographic data is summarized in Fig. 1, Fig. S4 and S5 and Tables S1–S3, ESI.† The radical **1** gave two types of crystals in one batch: a brown needle type and brown plate type. The needle-shaped crystal is the pure crystal of **1**, as shown in Fig. 1a and b. The crystal data was solved as a disordered structure due to the position of an oxy-radical unit. The dihedral angle between two-anthracene units is 70.1(2)°. The bond length at C8–C8′ is 1.492(3) Å, indicating a single bond. This is different from a stable 2,6-di-*tert*-butyl-4-(4′-nitrophenyl)phenoxyl (^{t}BuNPArO$^\bullet$) radical with an aryl–aryl bond length of 1.4754 Å and an aryl–aryl

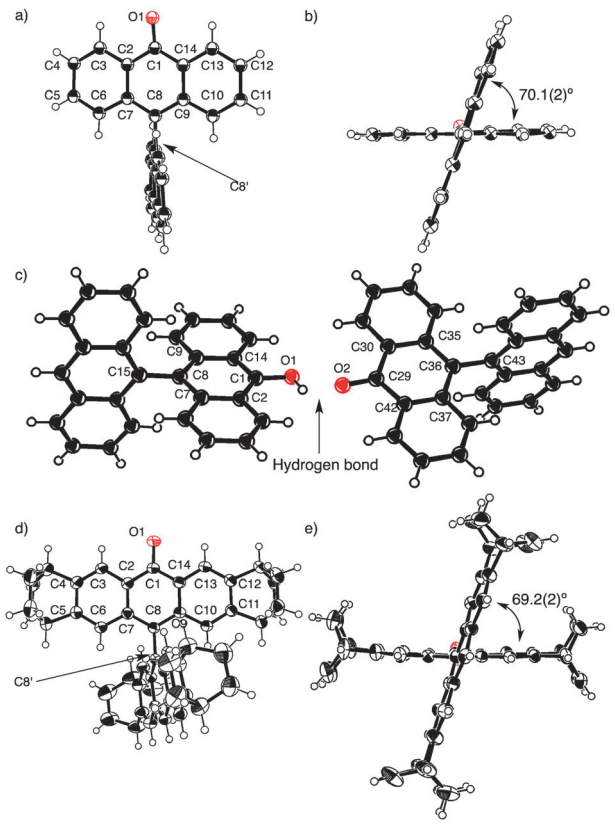

Fig. 1 Crystal structures of (a) top view; and (b) side view of **1**; (c) co-crystal with **1** and anthroxyl anthracene (**1-H**); (d) top view; and (e) side view of **2**. Solvent molecules are omitted for clarity. Thermal ellipsoids represent 50% probability.

torsion angle of 17.5°, where the spin density expanded the whole molecule.[5b] The crystal with the plate-shape contains 10-hydroxy-9,9′-anthyrylanthracene (**1-H**) and the radical **1** as a pair *via* [O–H···O$^\bullet$] hydrogen bonding (Fig. 1c, Fig. S4 and S5, ESI†) in the co-crystal. The compound **1-H** was obtained from **1** *in situ* during the crystallization. The bond length of O1–C1 of **1-H** is 1.364(3) Å, which confirms to a normal phenoxyl bond. The C–C bond lengths of **1-H** are those of typical aromatic C–C bonds and the bond length of C8–C15 for **1-H** is 1.496(3) Å. Thus, **1-H** in the co-crystal is 9,9′-anthryl-10-anthranol. The bond length of O2–C29 of **1** is 1.247(3) Å, which is 0.12 Å shorter than that of O1–C1 of **1-H**. The bond lengths of C29–C42, C29–C30, C35–C36, and C36–C37 are 1.457(3), 1.464(4), 1.425(3), and 1.425(7) Å, respectively, assigned to single bonds and the central ring next to O2 is not aromatic. The bond length of C36–C43 for **1** is 1.492(3) Å. The bond lengths of **1** suggest that the resonant structure E in Scheme 1 mainly contributes to the structure of radical **1**. The radical spin density should be higher at the 9-position and the steric protection of the most reactive carbon atom is effective in stabilizing the phenoxyl type radicals. The two anthryl units are orthogonal to each other with the mutual angles of 87.4(3)° for **1** and 89.1(3)° for **1-H**. The crystal structure of **2** shows a similar result to the needle-shaped crystal of **1** (Fig. 1d and e).[10] The crystal data was solved as a disordered structure due to the position of the oxy-radical unit. The two anthracene units are cross-shaped and the dihedral angle is 69.2(2)°. The C8–C8′ bond length that connects two anthracene skeletons is 1.498(3) Å. A co-crystal of **2** and **2-H** was not obtained.

The electronic structures of **1** and **2** were investigated by electron spin resonance (ESR) measurement. The ESR spectra of **1** and **2** in toluene are shown in Fig. 2, together with the simulation pattern. The signals of **1** are attributed to four positions in the anthroxyl skeleton, and the simulated hfccs are 0.90 (2H), 3.28 (2H), 0.90 (2H) and 3.28 G (2H). The *g*-value is 2.0023, which corresponds to a general organic free radical compound. The line width of the ESR spectrum of **2** was wider than that of **1** and the spectrum was hardly changed even by varying the temperature. The signals of **2** are ascribed to the two positions in the skeleton. The simulated hfccs are 1.00 (2H) and 2.80 G (2H) and the *g*-value is 2.0024. According to the spin density calculation (Fig. 2c and d), both **1** and **2** have the highest spin densities on C8 substituted with anthryl or the derivative (for numbering, see Fig. 1). This result suggests that the resonant structure E in Scheme 1 is also the main structure for **1** and **2** in solution. The anthryl groups are substantially orthogonal to the phenoxyl skeleton, contributing as steric protection to the radical. Density functional theory (DFT) calculations at the B3LYP/6-31G(d) level were conducted to provide further understanding of SOMO.[11] Computed spin densities showed that the unpaired electrons were delocalized on the anthroxyl skeleton for each compound rather than the substituent-acenes (Fig. S7, ESI†).

The UV-vis absorption spectra of **1** and **2** recorded in toluene are shown in Fig. 3a and Table 1. Each solution displayed a dark yellow color. The UV-vis absorption spectrum of **1** shows

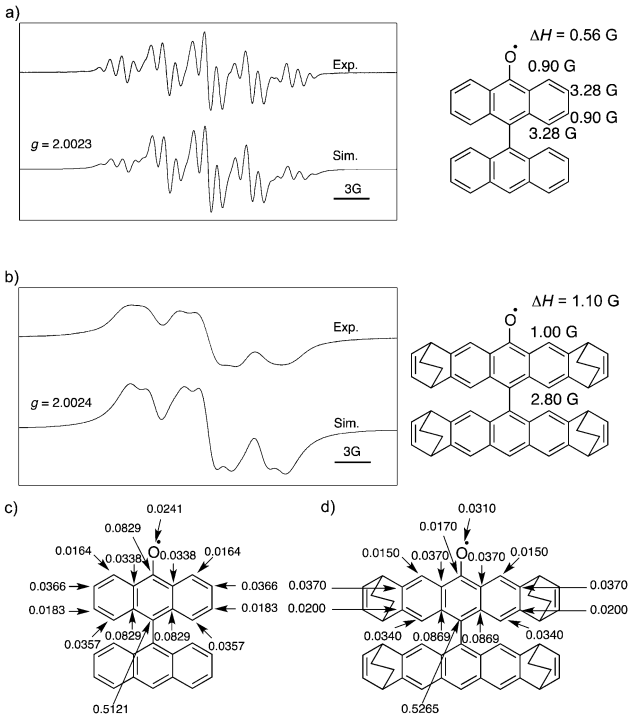

Fig. 2 ESR spectra and simulations of (a) **1** in toluene (1.6×10^{-2} mM) at 183 K and (b) **2** in toluene (2.7×10^{-2} mM) at 183 K. Spin density of (c) **1**; and (d) **2** computed at the B3LYP/6-31G(d) level.

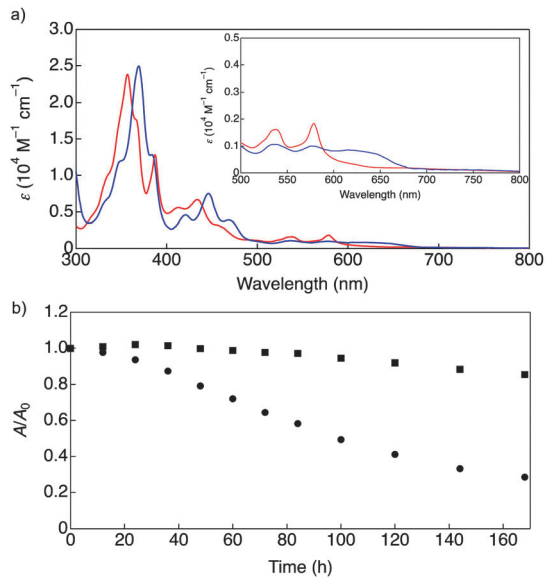

Fig. 3 (a) UV-vis absorption spectra of **1** (red line) and **2** (blue line) in toluene. (b) Decay profiles of UV-vis absorption spectra of (a) **1** (● 357 nm) and (b) **2** (■ 369 nm).

the major absorption at 357 (ε = 23 900 M^{-1} cm^{-1}) and 387 nm (ε = 12 900 M^{-1} cm^{-1}) and the minor absorption broadened to 800 nm with a maxima at 413 (ε = 5590 M^{-1} cm^{-1}), 434 (ε = 6660 M^{-1} cm^{-1}), 537 (ε = 1620 M^{-1} cm^{-1}) and 578 nm (ε = 1830 M^{-1} cm^{-1}). Because the UV-vis absorption spectrum of 9,9′-bianthryl is up to 400 nm,[12] the absorption wavelength is

Table 1 Summary of optical and electrochemical properties of radicals

Compd.	λ_{abs} [a] (nm)	E_{ox} [b] (V)	E_{red} [b] (V)
1	357, 387, 413, 434, 537, 578	0.55	−0.77
2	369, 384, 421, 446, 537, 576, 615	0.25, 0.91	−0.94

[a] In toluene. [b] The values were obtained by cyclic voltammetry. V *vs.* Fc/Fc^+.

red-shifted by the contribution of SOMO, as shown by the TD-DFT calculations (Fig. S8, ESI†). The BCOD-fused compound **2** displays an absorption spectrum with the red-shifted major absorption at 369 (ε = 25 000 M^{-1} cm^{-1}) and 384 (ε = 12 800 M^{-1} cm^{-1}) nm, and with the minor absorption broader and spread to 800 nm compared to those of **1**. The photo-stability of the radical in toluene was checked by UV-vis absorption spectral change. The solution was kept in room light under air and the temporal spectral change was measured, as shown in Fig. 3b, Fig. S9 and S10, ESI.† The peak-top (357 nm) of the absorbance of **1** is gradually decreased and the half life ($\tau_{1/2}$) is calculated to be 92 h. In contrast, $\tau_{1/2}$ of **2** was significantly longer than that of **1** and was estimated to be 274 h (11.4 d). The stability was improved about 3 times by inserting the BCOD moieties.

The electrochemical properties of the radicals were studied by cyclic voltammetry (CV) in dry dichloromethane containing 0.1 M tetra-*n*-butylammonium hexafluorophosphate ($n$$Bu_4NPF_6$) as a supporting electrolyte. The results are summarized in Table 1 and Fig. S11, ESI.† The one-electron reduction potentials ($E_{red}^{1/2}$ *vs.* Fc/Fc^+) of **1** and **2** are at −0.77 V and −0.94 V, respectively. The radical **1** shows one oxidation potential at 0.55 V (*vs.* Fc/Fc^+), whereas **2** shows two reversible oxidation waves at 0.25 and 0.91 V (*vs.* Fc/Fc^+). In comparison with **1**, the first oxidation and reduction potentials of compound **2** are shifted to the negative side. It is considered that the SOMO energy level of **2** rises by receiving the electric effect of σ–π hyperconjugation of BCOD-units to the anthracene moiety.[13] From CV and DFT calculations, the stability of **2** against electrochemical oxidation is predicted to be lower than that of **1**. The surrounding structures of the C8 position of **1** and **2** are similar in crystals due to the similarity of the angles of two anthryl planes and the C8–C8′ distances. However, the better stability of **2** in solution suggests the restricted freedom of rotation on the C8–C8′ axis for **2** compared to that for **1** owing to the BCOD substituents at the edge of the anthracene unit, thus restricting the reactivity of C8 to give a quinoid structure (Fig. S12, ESI†).

In conclusion, we were successful in preparing and characterizing stable 9,9′-anthryl-anthroxyl radicals.[14] The result of X-ray structural analysis, ESR spectra and DFT calculations suggested the highest spin density of radical **1** localized at the 9-position due to the resonance and the stabilization of the phenoxyl radical achieved by protection of the most reactive position with an anthryl group. The peripheral BCOD-substituents influenced the energy levels of SOMOs to be raised by σ–π hyperconjugation to encourage the electrochemical oxidation and the absorption spectrum to be red-shifted. Furthermore, the stability of radical **2** in solution was improved owing to the steric hindrance of the BCOD-moiety to restrict the

rotation around the C8–C8′ axis. Finally, we have tried to prepare 6,6′-penthryl-penthroxy radical (**7**) from **2** by a retro-Diels–Alder reaction.[8,15] Although the formation of a pentacene dimer was detected,[16] the ESR measurement of the product was not successful at present because the life-time of the product is much shorter than that of **1**.

The authors thank Ms Yoshiko Nishikawa in NAIST for the measurement of mass spectra, Mr Fumio Asanoma in NAIST for the measurement of ESR spectra, Mr Shouhei Katao in NAIST for the measurement of single-crystal structure analysis. This work was partly supported by Grants-in Aid (No. 22350083 and 26105004 to H.Y. and No. 26288038 to N.A.), the Green Photonics Project in NAIST and the program for promoting the enhancement of research universities in NAIST supported by MEXT. J.W. acknowledges financial support from Singapore MOE Tier 2 grant (MOE2014-T2-1-080).

Notes and references

1 R. Pummerer and F. Frankfurter, *Chem. Ber.*, 1914, **47**, 1472.
2 (*a*) R. W. Kreilick and S. I. Weissman, *J. Am. Chem. Soc.*, 1962, **84**, 306; (*b*) H.-J. Krüger, *Angew. Chem., Int. Ed.*, 1999, **38**, 627; (*c*) S. Itoh, M. Taki and S. Fukuzumi, *Coord. Chem. Rev.*, 2000, **198**, 3; (*d*) C. T. Lyons and T. D. P. Stack, *Coord. Chem. Rev.*, 2013, **257**, 528.
3 (*a*) E. Müller, A. Schick and K. Scheffler, *Chem. Ber.*, 1959, **92**, 474; (*b*) E. R. Altwicker, *Chem. Rev.*, 1967, **67**, 475; (*c*) V. W. Manner, T. F. Markle, J. H. Freudenthal, J. P. Roth and J. M. Mayer, *Chem. Commun.*, 2008, 256; (*d*) J. M. Wittman, R. Hayoun, W. Kaminsky, M. K. Coggins and J. M. Mayer, *J. Am. Chem. Soc.*, 2013, **135**, 12956.
4 (*a*) A. Sokolowski, J. Müller, T. Weyhermüller, R. Schnepf, P. Hildebrandt, K. Hildenbrand, E. Bothe and K. Wieghardt, *J. Am. Chem. Soc.*, 1997, **119**, 8889; (*b*) A. Philibert, F. Thomas, C. Philouze, S. Hamman, E. Saint-Aman and J.-L. Pierre, *Chem. – Eur. J.*, 2003, **9**, 3803; (*c*) Y. Shimazaki, S. Huth, S. Karasawa, S. Hirota, Y. Naruta and O. Yamauchi, *Inorg. Chem.*, 2004, **43**, 7816.
5 (*a*) C. Xie, P. M. Lahti and C. George, *Org. Lett.*, 2000, **2**, 3417; (*b*) T. R. Porter, W. Kaminsky and J. M. Mayer, *J. Org. Chem.*, 2014, **79**, 9451.
6 (*a*) J. Cai, P. Ruffieux, R. Jaafar, M. Bieri, T. Braun, S. Blankenburg, M. Muoth, A. P. Seitsonen, M. Saleh, X. Feng, K. Müllen and R. Fasel, *Nature*, 2010, **466**, 470; (*b*) L. Chen, Y. Hernandez, X. Feng and K. Müllen, *Angew. Chem., Int. Ed.*, 2012, **51**, 7640; (*c*) A. Konishi, Y. Hirao, K. Matsumoto, H. Kurata, R. Kishi, Y. Shigeta, M. Nakano, K. Tokunaga, K. Kamada and T. Kubo, *J. Am. Chem. Soc.*, 2013, **135**, 1430.
7 L. S. Singer, I. C. Lewis, T. Richerzhagen and G. Vincow, *J. Phys. Chem.*, 1971, **75**, 290.
8 K. Tanaka, N. Aratani, D. Kuzuhara, S. Sakamoto, T. Okujima, N. Ono, H. Uno and H. Yamada, *RSC Adv.*, 2013, **3**, 15310.
9 (*a*) S. M. Arabei and T. A. Pavich, *J. Appl. Spectrosc.*, 2000, **67**, 236; (*b*) X. Zhang, J. Li, H. Qu, C. Chi and J. Wu, *Org. Lett.*, 2010, **12**, 3946.
10 The single crystals of **2** from chloroform/methanol also gave crystal of **2**, but not co-crystal like **1** and **1H** (Fig. S6 and Table S4, ESI†). CCDC number is 1042904.
11 M. J. Frisch, *et al.*, *Gaussian 09, Revision D.01*, see the ESI† for details.
12 P. Natarajan and M. Schmittel, *J. Org. Chem.*, 2013, **78**, 10383.
13 (*a*) K. Komatsu, H. Akamatsu, Y. Jinbu and K. Okamoto, *J. Am. Chem. Soc.*, 1988, **110**, 633; (*b*) A. Matsuura, T. Nishinaga and K. Komatsu, *J. Am. Chem. Soc.*, 2000, **122**, 10007.
14 Whilst this work was under consideration, the following manuscript was published: Y. Hirao, T. Saito and T. Kubo, *Angew. Chem., Int. Ed.*, 2015, **54**, 2402.
15 (*a*) S. Ito, T. Murashima, N. Ono and H. Uno, *Chem. Commun.*, 1998, 1661; (*b*) H. Yamada, T. Okujima and N. Ono, *Chem. Commun.*, 2008, 2957.
16 The weight loss in thermogravimetric analysis of **2** (Fig. S13, ESI†) starts at 200 °C and ends around 300 °C, but soon the weight loss started again. The preparation of radical **7** was tried by heating by microwave in ethyleneglycol at 300 °C for 5 min under argon atmosphere. After the quick filtration, the precipitate was suggested to have pentacene dimer unit by APCI-mass measurement (Fig. S14, ESI†).